

COMBINED INTERPRETATION OF B -PHYSICS ANOMALIES AND MODEL BUILDING* **

DAVID MARZOCCA

INFN, Sezione di Trieste, SISSA, Via Bonomea 265, 34136 Trieste, Italy

(Received April 20, 2018)

The observed anomalies in semileptonic B -meson decays represent the most significant deviation from the SM observed to date in particle physics. In this paper, I discuss how these can be consistently combined in a coherent and simple EFT setup. The complete set of heavy states which can generate the required operators when integrated out is then presented: colourless vectors, vector leptoquarks and scalar leptoquarks. Among these, the leptoquarks offer the most compelling case and their most interesting signatures in high- p_T searches are explored.

DOI:10.5506/APhysPolB.49.1279

1. Introduction

The largest set of deviations from the Standard Model (SM) observed in the last few years in particle physics experiments are the numerous hints of Lepton Flavour Universality (LFU) violations observed in semi-leptonic B decays. The first class of deviations has been observed in charged-current $b \rightarrow c\tau^-\bar{\nu}$ transitions via the $R(D)$ and $R(D^*)$ observables [2–5]. The deviation from the tree-level SM contribution is at the level of $\sim 20\%$ with a combined significance of $\sim 4\sigma$. The second class of anomalies occurs instead in flavour-changing neutral-current transitions $b \rightarrow s\ell^+\ell^-$ [6–9]. Also, in this case, all the observed deviations can be consistently combined, the deviation from the loop-suppressed SM contribution is $\sim 10\%$ at the amplitude level and the global significance is above the 4σ level [10, 11].

These deviations from the SM have triggered a series of theoretical speculations about the possible new physics (NP) interpretations. Attempts to provide a combined/coherent explanation for both charged- and neutral-current anomalies have been presented in Refs. [1, 12–35]. One of the puzzling aspects of the present anomalies is that they have been observed only

* Presented at the Cracow Epiphany Conference on Advances in Heavy Flavour Physics, Kraków, Poland, January 9–12, 2018.

** This paper is based on Ref. [1].

in semi-leptonic B decays and the size of the effect is quite large compared to the corresponding SM amplitude. On the other hand, no deviation from the SM has been seen so far in the precise (per-mil) tests of LFU in electroweak precision tests, τ decays and semi-leptonic K and π decays. A possible solution to this issue is to assume that the NP mainly couples to third generation fermions of quarks and leptons, with a smaller mixing with light generations [14, 26, 36]. This feature can be naturally explained for example by introducing a $SU(2)_q \times SU(2)_\ell$ flavour symmetry [37, 38]. In this case, the scale of the mediators responsible for the observed deviations should be close to the ~ 1 TeV scale. This creates possible challenges to be consistent with the absence of NP signals from high- p_T data from the LHC [39] and other low-energy precision observables such as electroweak precision measurements [40, 41] and B_s and B_d meson–antimeson mixing.

In this proceedings, based on Ref. [1], I present a combined Effective Field Theory (EFT) analysis of the observed deviations from the SM as well as all the other available constraints from low-energy physics and electroweak precision tests. The required set of operators can be generated by integrating out at the tree-level some heavy states. I present the complete list of such particles via a simplified model approach, allowing to connect low-energy data with high- p_T observables.

2. Semi-leptonic effective operators

In this section, we study the phenomenology of the semileptonic effective operators at the electroweak scale employing the formalism of the SM EFT. For both charged- and neutral-current anomalies, semileptonic operators involving only left-handed fermions offer the best fit. For this reason, we focus on the two possible such operators, with a flavour structure determined by the $U(2)_q \times U(2)_\ell$ flavour symmetry, minimally broken by two spurions $V_q \sim (\mathbf{2}, \mathbf{1})$ and $V_\ell \sim (\mathbf{1}, \mathbf{2})$ [37, 38].

2.1. The effective Lagrangian

We consider the following effective Lagrangian at the NP scale Λ

$$\mathcal{L}_{\text{eff}} = \mathcal{L}_{\text{SM}} - \frac{1}{v^2} \lambda_{ij}^q \lambda_{\alpha\beta}^\ell \times \left[C_T \left(\bar{Q}_L^i \gamma_\mu \sigma^a Q_L^j \right) \left(\bar{L}_L^\alpha \gamma^\mu \sigma^a L_L^\beta \right) + C_S \left(\bar{Q}_L^i \gamma_\mu Q_L^j \right) \left(\bar{L}_L^\alpha \gamma^\mu L_L^\beta \right) \right], \quad (1)$$

where $v \approx 246$ GeV. For simplicity, the definition of the EFT cut-off scale and the normalisation of the two operators is reabsorbed in the flavour-blind adimensional coefficients C_S and C_T . We adopt as reference flavour basis the down-type quark and charged-lepton mass eigenstate basis, where

$Q_L^i = (V_{ji}^* u_L^j, d_L^i)^T$ and $L_L^\alpha = (\nu_L^\alpha, \ell_L^\alpha)^T$. The flavour structure in Eq. (1) is contained in the Hermitian matrices λ_{ij}^q , $\lambda_{\alpha\beta}^\ell$ and follows from the assumed $U(2)_q \times U(2)_\ell$ flavour symmetry and its breaking [1]

$$\lambda_{bb}^q = \lambda_{\tau\tau}^\ell = 1, \quad \lambda_{sb}^q = \mathcal{O}(|V_{cb}|), \quad \left| \lambda_{\tau\mu}^\ell \right| \ll 1, \quad \lambda_{\mu\mu}^\ell = \mathcal{O} \left(\left(\lambda_{\tau\mu}^\ell \right)^2 \right). \quad (2)$$

2.2. Fit of the semi-leptonic operators

To quantify how well the proposed framework can accommodate the observed anomalies, we perform a fit to low-energy data with four free parameters: C_T , C_S , λ_{sb}^q , and $\lambda_{\mu\mu}^\ell$, while for simplicity we set $\lambda_{\tau\mu}^\ell = 0$ ¹. The set of experimental measurements entering the fit, together with their functional dependence on the fit parameters, is discussed in length in Ref. [1] and summarised in Table I.

TABLE I

Observables entering in the fit, together with the associated experimental bounds (assuming the uncertainties follow the Gaussian distribution) and their linearised expressions in terms of the EFT parameters.

Observable	Experimental bound	Linearised expression
$R_{D^{(*)}}^{\tau\ell}$	1.237 ± 0.053	$1 + 2C_T (1 - \lambda_{sb}^q V_{tb}^*/V_{ts}^*) (1 - \lambda_{\mu\mu}^\ell/2)$
$\Delta C_9^\mu = -\Delta C_{10}^\mu$	-0.61 ± 0.12 [42]	$-\frac{\pi}{\alpha_{\text{em}} V_{tb} V_{ts}^*} \lambda_{\mu\mu}^\ell \lambda_{sb}^q (C_T + C_S)$
$R_{b \rightarrow c}^{\mu e} - 1$	0.00 ± 0.02	$2C_T (1 - \lambda_{sb}^q V_{tb}^*/V_{ts}^*) \lambda_{\mu\mu}^\ell$
$B_{K^{(*)} \nu \bar{\nu}}$	0.0 ± 2.6	$1 + \frac{2}{3} \frac{\pi}{\alpha_{\text{em}} V_{tb} V_{ts}^*} C_{\text{SM}}^{\nu\nu} (C_T - C_S) \lambda_{sb}^q (1 + \lambda_{\mu\mu}^\ell)$
$\delta g_{\tau_L}^Z$	-0.0002 ± 0.0006	$0.033C_T - 0.043C_S$
$\delta g_{\nu_\tau}^Z$	-0.0040 ± 0.0021	$-0.033C_T - 0.043C_S$
$ g_\tau^W/g_\ell^W $	1.00097 ± 0.00098	$1 - 0.084C_T$
$\mathcal{B}(\tau \rightarrow 3\mu)$	$(0.0 \pm 0.6) \times 10^{-8}$	$2.5 \times 10^{-4} (C_S - C_T)^2 (\lambda_{\tau\mu}^\ell)^2$

We minimise the total χ^2 function to find the best-fit point and the corresponding confidence level intervals. The results are presented as 2D plots after marginalising over the other two parameters in figure 1. The main observations can be summarised as follows:

- The radiative constraints from electroweak precision tests and τ decays favour sizeable values of $\lambda_{sb}^q/V_{ts}^* \approx -\lambda_{sb}^q/V_{cb}$, which allow to lower the

¹ We explicitly verified that a non-zero $\lambda_{\tau\mu}^\ell$ has no impact on the fit results.

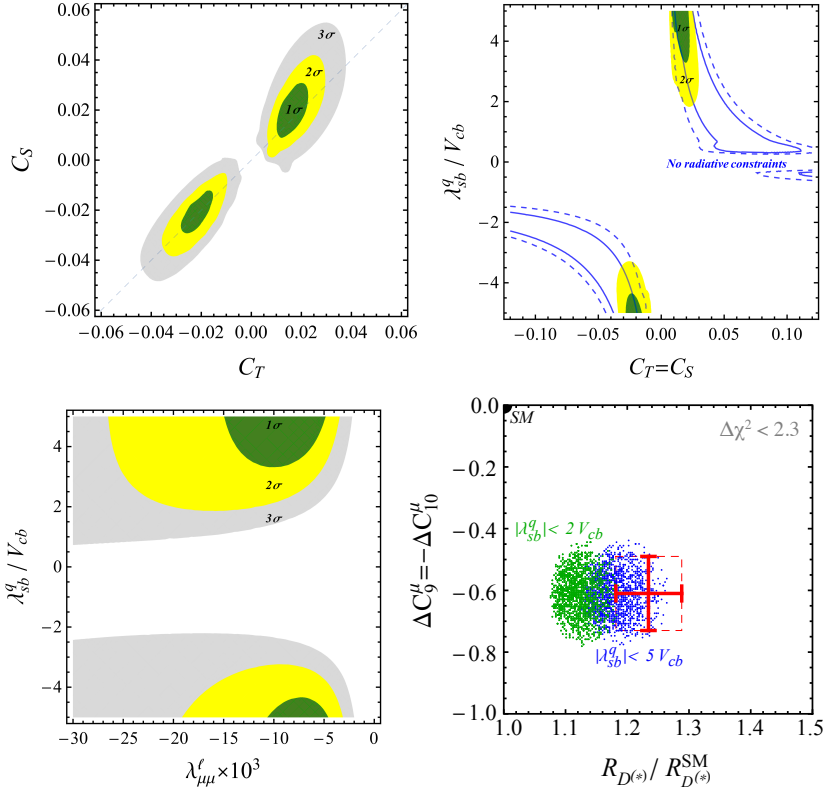


Fig. 1. (Colour on-line) Fit to the semi-leptonic and purely leptonic (radiatively generated) observables in Table I, in the framework of the triplet and singlet $V-A$ operators (see Eq. (1)), imposing $|\lambda_{sb}^q| < 5|V_{cb}|$. In dark grey/green, light grey/yellow, and grey, we show the $\Delta\chi^2 \leq 2.3$ (1σ), 6.2 (2σ), and 11.8 (3σ) regions, respectively, after marginalising over all other parameters. In the top right plot, we fix $C_T = C_S$ and perform a fit with and without the radiatively induced observables. In the bottom right plot, we show the 1σ prediction for $\Delta C_9^\mu = -\Delta C_{10}^\mu$ (following from $R_{K^{(*)}}^{\mu e}$ and $R_{D^{(*)}}^{\tau \ell}$). The black/red cross denotes the 1σ experimental constraint.

value of $C_{T,S}$ (*i.e.* to increase the scale of NP) keeping fixed the contribution to $R_{D^{(*)}}^{\tau \ell}$ (see the top right panel of Fig. 1). Having a large NP scale also helps when confronting the simplified models with the high- p_T searches.

- In this *large mixing* region, a too large effect in $\mathcal{B}(B \rightarrow K^* \nu \bar{\nu})$ is alleviated by requiring $C_T \sim C_S$. The degree to which this relation should be satisfied can be seen in the top left panel of Fig. 1 and is at the 30% level. This also eases the bound from $Z\tau\tau$ couplings.

- The measured value of $\Delta C_9^\mu = -\Delta C_{10}^\mu$, together with the size of λ_{sb}^q and $C_{T,S}$ from the points above, requires a value of $\lambda_{\mu\mu}^\ell \approx -\mathcal{O}(10^{-2})$, *i.e.* $\lambda_{\tau\mu} \sim \mathcal{O}(0.1)$. This value of $\lambda_{\tau\mu}$ is also consistent with limits from LFV in τ decays.
- The best-fit region is consistent with both $R_{K^{(*)}}^{\mu e}$ and $R_{D^{(*)}}^{\tau\ell}$ anomalies. In the bottom right panel of Fig. 1, we show the values of the two observables for a randomly chosen set of points within the 1σ preferred region ($\Delta\chi^2 < 2.3$). Larger values of $|\lambda_{sb}^q|$ help to improve the fit to $R_{D^{(*)}}^{\tau\ell}$.

The smoking gun of the preferred solution of the EFT fit is a huge enhancement of $b \rightarrow s\tau\bar{\tau}$ transitions between two and three orders of magnitude with respect to the SM. The size of the enhancement is correlated with the maximal allowed value of λ_{bs} .

3. Simplified models

In this section, we study three specific (simplified) UV scenarios with explicit mediators. We take the simplifying assumption that only one or two of these mediators are present and with the couplings required to generate the singlet and triplet operators. It should be kept in mind that in more complete theories a more complex scenario might arise, where also other states and/or other coupling structures might be present.

The complete set of single-mediator models with tree-level matching to the effective operators in Eq. (1) consists of [43]:

Field	Spin	$SU(3)_c$	$SU(2)_L$	$\mathcal{U}(1)_Y$	
B'_μ	1	1	1	0	
W'_μ	1	1	3	0	
U_1^μ	1	3	1	2/3	(3)
U_3^μ	1	3	3	2/3	
S_1	0	$\bar{3}$	1	1/3	
S_3	0	$\bar{3}$	3	1/3	

The first two are colourless vectors, while all the others are leptoquark (LQ) fields, *i.e.* they couple to currents made of one quark and one lepton. In figure 2, we show the correlation between triplet and singlet operators predicted in all single-mediator models, compared to the regions favoured by the EFT fit. Note that for the LQ, only one sign of the coefficients is allowed since it is proportional to the modulus squared of the relevant coupling, as is shown in detail below.

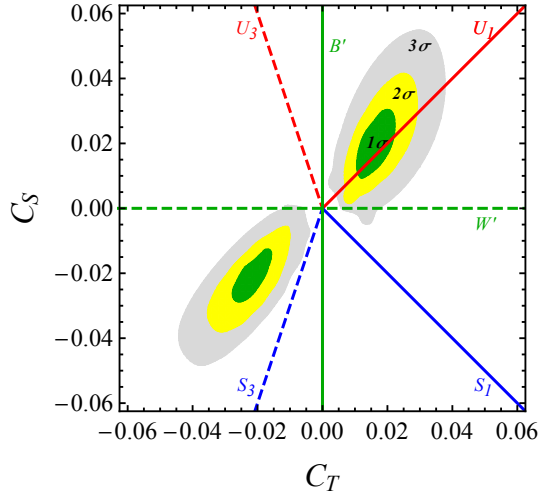


Fig. 2. (Colour on-line) The lines show the correlations among triplet and singlet operators in single-mediator models. Colourless vectors are shown in green, coloured scalar in blue, while coloured vectors in red. Electroweak singlet mediators are shown with the solid lines, while triplets with dashed.

3.1. Scenario I: Vector leptoquark

The plot in figure 2 clearly singles out the case of a $SU(2)_L$ -singlet vector LQ, $U_1^\mu \equiv (\mathbf{3}, \mathbf{1}, 2/3)$ as the best single-mediator case. This UV realisation was originally proposed in [18]. Its interaction to the left-handed quarks and leptons is described by the Lagrangian

$$\mathcal{L}_U \supset g_U \beta_{i\alpha} (\bar{Q}_i \gamma^\mu L_\alpha) U_{1,\mu} + \text{h.c.} \tag{4}$$

Here, $\beta_{i\alpha}$ describe the flavour structure of the couplings, which can be related to the one introduced in Eq. (2)

$$\beta_{b\tau} \equiv 1, \quad \beta_{s\tau} \sim \lambda_{bs}, \quad \beta_{b\mu} \sim \lambda_{\tau\mu}, \quad \beta_{s\mu} \sim \lambda_{bs} \lambda_{\tau\mu}. \tag{5}$$

After integrating out the leptoquark field, the tree-level matching condition for the EFT is

$$\begin{aligned} \mathcal{L}_{\text{eff}} \supset & -\frac{1}{v^2} C_U \beta_{i\alpha} \beta_{j\beta}^* \\ & \times \left[\left(\bar{Q}_L^i \gamma_\mu \sigma^a Q_L^j \right) \left(\bar{L}_L^\beta \gamma^\mu \sigma^a L_L^\alpha \right) + \left(\bar{Q}_L^i \gamma_\mu Q_L^j \right) \left(\bar{L}_L^\beta \gamma^\mu L_L^\alpha \right) \right], \end{aligned} \tag{6}$$

where $C_U = v^2 |g_U|^2 / (2M_U^2) > 0$. Note that in this case, the singlet and triplet operators have the same flavour structure and, importantly, the relation $C_S = C_T$ is automatically fulfilled at the tree-level. Furthermore,

as already stressed, the flavour-blind contraction involving light fermions (flavour doublets) is automatically forbidden by the $U(2)_q \times U(2)_\ell$ symmetry. Last but not least, this LQ representation does not allow baryon number violating operators of dimension four. The best fit points described in Section 2.2 can be recovered without any tuning of the model parameters.

Another welcome feature of the vector leptoquark is the absence of a tree-level contribution to $B_{s(d)}$ meson–antimeson mixing. However, a contribution is generated at the one-loop level. The result of the loop is quadratically divergent and, therefore, strongly dependent on the UV completion. Furthermore, in most models providing a UV-completion of the vector leptoquark, neutral vectors are present which, in turn, can mediate $\Delta F = 2$ processes at the tree level, which require a tuning or a deviation from the pure $U(2)_q$ expectations of the model’s parameters [25, 31, 32, 34, 35].

3.2. Scenario II: Scalar leptoquarks

From figure 2, one concludes that a single scalar leptoquark cannot reproduce the result of the EFT fit. However, by introducing both scalar leptoquarks $S_1 = (\mathbf{3}, \mathbf{1}, 1/3)$ and $S_3 = (\mathbf{3}, \mathbf{3}, 1/3)$, this becomes easily possible. This might also be naturally justified in more UV complete descriptions if both representations arise as partners, with the same underlying mechanism. The relevant interaction Lagrangian is given by [43]

$$\mathcal{L} \supset g_1 \beta_{1,i\alpha} (\bar{Q}_L^c \epsilon L_L^\alpha) S_1 + g_3 \beta_{3,i\alpha} (\bar{Q}_L^c \epsilon \sigma^a L_L^\alpha) S_3^a + \text{h.c.}, \tag{7}$$

where $\epsilon = i\sigma^2$, $Q_L^c = C\bar{Q}_L^T$, and S_3^a are the components of the S_3 leptoquark in $SU(2)_L$ space. Contrary to the vector LQ case, baryon number conservation is not automatically absent in the renormalisable operators built in terms of $S_{1,3}$ and must be imposed as an additional symmetry of the theory.

Integrating out the leptoquark states at tree-level and matching to the effective theory, we find the following semi-leptonic operators:

$$\begin{aligned} \mathcal{L}_{\text{eff}} \supset & -\frac{1}{v^2} (C_1 \beta_{1,i\beta} \beta_{1,j\alpha}^* - C_3 \beta_{3,i\beta} \beta_{3,j\alpha}^*) \left(\bar{Q}_L^i \gamma_\mu \sigma^a Q_L^j \right) \left(\bar{L}_L^\alpha \gamma^\mu \sigma^a L_L^\beta \right) \\ & -\frac{1}{v^2} (-C_1 \beta_{1,i\beta} \beta_{1,j\alpha}^* - 3C_3 \beta_{3,i\beta} \beta_{3,j\alpha}^*) \left(\bar{Q}_L^i \gamma_\mu Q_L^j \right) \left(\bar{L}_L^\alpha \gamma^\mu L_L^\beta \right), \end{aligned} \tag{8}$$

where $C_{1,3} = v^2 |g_{1,3}|^2 / (4M_{S_{1,3}}^2) > 0$. Enforcing a minimally broken $U(2)_q \times U(2)_\ell$ flavour symmetry, the two mixing matrices $\beta_{1,i\alpha}$ and $\beta_{3,i\alpha}$ follow a very similar structure as the vector LQ case, Eq. (5). These two flavour matrices are, in general, different. However, for the sake of simplicity, in the fit we fix $\beta_{3,s\mu} = \beta_{1,s\mu}$ and $\beta_{1,b\mu} = \beta_{3,b\mu}$, keeping only the two s – τ elements different (since this is also required for the fit to work). The leading contributions to

the flavour observables in Table I are

$$\begin{aligned}
 R_{D^{(*)}}^{\tau/\ell} &\approx 1 + 2(C_1 - C_3) + 2(C_1\beta_{1,s\tau} - C_3\beta_{3,s\tau})\frac{V_{cs}}{V_{cb}}, \\
 \Delta C_9 &= -\Delta C_{10} = \frac{4\pi}{\alpha V_{tb}V_{ts}}C_3\beta_{s\mu}\beta_{b\mu}, \\
 R_{b\rightarrow c}^{\mu/e} &\approx 1 + 2(C_1 - C_3)\beta_{b\mu}\left(\beta_{b\mu} + \beta_{s\mu}\frac{V_{cs}}{V_{cb}}\right), \\
 B_{K^*\nu\nu} - 1 &\propto (C_1\beta_{1,s\tau} + C_3\beta_{3,s\tau}), \tag{9}
 \end{aligned}$$

see Ref. [1] for more detailed expressions. As for the vector LQ case, also with the two scalars it is possible to completely recover the EFT fit solution without any tuning [1]

$$\begin{aligned}
 C_1 &\approx C_3 \lesssim 10^{-2}, & \beta_{1,s\tau} &\approx -\beta_{3,s\tau} \approx (\text{few}) \times |V_{ts}| > 0, \\
 \beta_{1(3),b\mu} &\approx 0.1, & \beta_{1(3),s\mu} &\approx \beta_{1(3),b\mu}\beta_{1,s\tau}. \tag{10}
 \end{aligned}$$

The greatest virtue of this scenario is the natural absence of significant constraints from $\Delta F = 2$ processes due to the smallness of the corresponding (finite) loop amplitudes.

3.3. Scenario III: Colourless vectors

The last simplified model we consider includes the pair of heavy colourless vectors, W'_μ and B'_μ , coupled respectively to the SM fermion triplet and singlet currents (see [1, 14] for the details). By integrating out these vector fields, one generates at the tree-level the triplet and singlet semileptonic operators of the EFT fit described above, but also four-quark and four-lepton operators. While the observables described in Section 2 can be easily reproduced, inserting the required parameters, one gets contributions to $\Delta B = 2$ and $\Delta C = 2$ amplitudes larger than the experimental limits by a factor of ~ 500 and ~ 20 , respectively [1]. When taken at face value, these observables exclude this scenario as a viable explanation of the flavour anomalies.

An alternative way in which the model could survive is to abandon the large mixing region selected by the EFT fit and move to the small λ_{sb}^q region, where $\lambda_{sb}^q = \mathcal{O}(10^{-1}) \times |V_{cb}|$. The most serious problem of this scenario, already encountered in Ref. [14], is the fact that the required large values of $\epsilon_{\ell,q}$ imply a low mass scale and large coupling of the neutral triplet vector resonance to $b_L b_L$ and $\tau_L \tau_L$. Therefore, the very stringent limits from high- p_T di-tau searches apply [39] and can be avoided only if the resonances have a very large width [14, 39].

4. Direct searches of leptoquarks

The vector and scalar LQ can be pair produced at the LHC via their QCD interactions. The vector LQ U_1^μ is expected to decay to $t\bar{\nu}_\tau$ and $b\tau^+$ final states democratically, while the scalars decay to: ($S_3^{Q=4/3} \rightarrow \bar{b}\tau^+$), ($S_1, S_3^{Q=1/3} \rightarrow \bar{t}\tau^+, \bar{b}\bar{\nu}_\tau$), and ($S_3^{Q=-2/3} \rightarrow \bar{t}\bar{\nu}_\tau$).

Presently, pair production offers the most stringent limits. A CMS search at 13 TeV with 12.9 fb^{-1} [44] implies $M_U > 1.0 \text{ TeV}$ or $M_{S_1} > 855 \text{ GeV}$, while the CMS recast of SUSY stop searches [45] implies $M_{S_3} > 1020 \text{ GeV}$ (via the $t\nu$ channel). For masses larger than approximately 1.4 TeV, the single production channel becomes more sensitive [1, 46]. Another relevant collider signature is the production of tau-lepton pairs at high energies ($pp \rightarrow \tau\bar{\tau} + X$) due to the t -channel (tree-level) leptoquark exchange [39]. Collider signatures involving muons in the final state [47] can be relevant in the future for large values of the $\beta_{b\mu}$ parameter

The compilation of the leading collider bounds, as well as the corresponding projections for 300 fb^{-1} , is shown in figure 3 for the vector LQ case. The preferred range of C_U from the flavour fit is translated to the green (1σ) and yellow (2σ) bands.

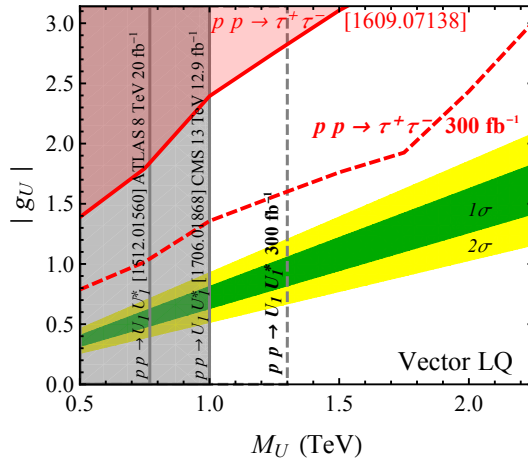


Fig. 3. (Colour on-line) Present and future-projected LHC constraints on the vector leptoquark model of Section 3.1. The 1σ and 2σ preferred regions from the low-energy fit are shown in green and yellow, respectively.

5. Conclusions

In this paper, based on Ref. [1], we presented an attempt to provide a coherent BSM interpretation of the *B*-physics anomalies which appeared in the last few years. By studying the problem at the EFT level, we showed that

a coherent solution can be found also while keeping into account the strong indirect constraints from electroweak precision tests and lepton flavour universality in τ decays. The solution points towards NP coupled mainly to third generation fermions, with a sizable 3–2 mixing in the quark sector, and an overall new physics scale of 1–2 TeV (with couplings of $\mathcal{O}(1)$).

Going beyond the EFT approach, we introduced the complete set of tree-level mediators which can generate the required singlet and triplet semileptonic operators: colourless vectors (triplet and singlets), vector leptoquarks and scalar leptoquarks. While the colourless vectors are excluded by a too large tree-level contribution to $\Delta F = 2$ processes, the leptoquarks are very good candidates to explain the observed anomalies.

Among these, the vector LQ U_1^μ is particularly interesting since it allows to fit all the observed deviations with one single mediators and very few parameters. Instead, both scalar leptoquarks S_1 and S_3 are required to perform the same goal. On the other hand, the latter solution could offer an easier way to avoid the strong $\Delta F = 2$ constraints once a full UV completion is introduced, since vector LQ are usually accompanied by colourless singlets which mediate it at the tree-level.

Presently, these third generation LQs are searched for at the LHC mainly via pair production, and the present limits are near the ~ 1 TeV scale, or in the $\tau\tau$ final state where they contribute in the t -channel. While it is not assured that they will ever be seen at the LHC, in particular if their mass will be large, it is extremely important to continue these LQ searches.

The data that will be collected and analysed by the LHCb and Belle II experiments in the next few years will give us a final answer on the nature of the B -physics anomalies. If they are confirmed as genuine new physics effects, a revolution of our understanding of physics at the TeV scale will take place, possibly with important implications also in our understanding of the SM flavour puzzle. The connection with UV models explored here will be crucial to test this NP in the high-energy frontier.

I thank the organisers of the Epiphany Conference for the very interesting conference and the pleasant stay in Kraków. I am also extremely grateful to D. Buttazzo, A. Greljo and G. Isidori for the collaboration for the work presented here.

REFERENCES

- [1] D. Buttazzo, A. Greljo, G. Isidori, D. Marzocca, *J. High Energy Phys.* **1711**, 044 (2017).
- [2] J.P. Lees *et al.*, *Phys. Rev. D* **88**, 072012 (2013).

- [3] S. Hirose *et al.*, *Phys. Rev. Lett.* **118**, 211801 (2017) [arXiv:1612.00529 [hep-ex]].
- [4] R. Aaij *et al.*, *Phys. Rev. Lett.* **115**, 111803 (2015) [*Addendum ibid.* **115**, 159901 (2015)].
- [5] A.R. Vidal, CERN EP Seminar, 06 June 2017.
- [6] R. Aaij *et al.*, *Phys. Rev. Lett.* **111**, 191801 (2013).
- [7] R. Aaij *et al.*, *J. High Energy Phys.* **1602**, 104 (2016).
- [8] R. Aaij *et al.*, *Phys. Rev. Lett.* **113**, 151601 (2014).
- [9] R. Aaij *et al.*, *J. High Energy Phys.* **1708**, 055 (2017) [arXiv:1705.05802 [hep-ex]].
- [10] W. Altmannshofer, D.M. Straub, Implications of $b \rightarrow s$ Measurements, in: Proc. of 50th Rencontres de Moriond Electroweak Interactions and Unified Theories, La Thuile, Italy, March 14–21, 2015, pages 333–338 [arXiv:1503.06199 [hep-ph]].
- [11] S. Descotes-Genon, L. Hofer, J. Matias, J. Virto, *J. High Energy Phys.* **1606**, 092 (2016).
- [12] B. Bhattacharya, A. Datta, D. London, S. Shivashankara, *Phys. Lett. B* **742**, 370 (2015).
- [13] R. Alonso, B. Grinstein, J. Martin Camalich, *J. High Energy Phys.* **1510**, 184 (2015).
- [14] A. Greljo, G. Isidori, D. Marzocca, *J. High Energy Phys.* **07**, 142 (2015).
- [15] L. Calibbi, A. Crivellin, T. Ota, *Phys. Rev. Lett.* **115**, 181801 (2015).
- [16] M. Bauer, M. Neubert, *Phys. Rev. Lett.* **116**, 141802 (2016).
- [17] S. Fajfer, N. Košnik, *Phys. Lett. B* **755**, 270 (2016).
- [18] R. Barbieri, G. Isidori, A. Pattori, F. Senia, *Eur. Phys. J. C* **76**, 67 (2016).
- [19] D. Das, C. Hati, G. Kumar, N. Mahajan, *Phys. Rev. D* **94**, 055034 (2016).
- [20] S.M. Boucenna *et al.*, *J. High Energy Phys.* **12**, 059 (2016).
- [21] D. Bečirević, S. Fajfer, N. Košnik, O. Sumensari, *Phys. Rev. D* **94**, 115021 (2016).
- [22] G. Hiller, D. Loose, K. Schoenwald, *J. High Energy Phys.* **1612**, 027 (2016).
- [23] B. Bhattacharya *et al.*, *J. High Energy Phys.* **01**, 015 (2017).
- [24] D. Buttazzo, A. Greljo, G. Isidori, D. Marzocca, *J. High Energy Phys.* **1608**, 035 (2016).
- [25] R. Barbieri, C.W. Murphy, F. Senia, *Eur. Phys. J. C* **77**, 8 (2017).
- [26] M. Bordone, G. Isidori, S. Trifinopoulos, *Phys. Rev. D* **96**, 015038 (2017) [arXiv:1702.07238 [hep-ph]].
- [27] A. Crivellin, D. Müller, T. Ota, *J. High Energy Phys.* **1709**, 040 (2017) [arXiv:1703.09226 [hep-ph]].
- [28] D. Bečirević, N. Košnik, O. Sumensari, R. Zukanovich Funchal, *J. High Energy Phys.* **1611**, 035 (2016).

- [29] Y. Cai, J. Gargalionis, M.A. Schmidt, R.R. Volkas, *J. High Energy Phys.* **1710**, 047 (2017) [arXiv:1704.05849 [hep-ph]].
- [30] E. Megías, M. Quiros, L. Salas, *J. High Energy Phys.* **1707**, 102 (2017) [arXiv:1703.06019 [hep-ph]].
- [31] R. Barbieri, A. Tesi, *Eur. Phys. J. C* **78**, 193 (2018) [arXiv:1712.06844 [hep-ph]].
- [32] L. Di Luzio, A. Greljo, M. Nardecchia, *Phys. Rev. D* **96**, 115011 (2017).
- [33] L. Calibbi, A. Crivellin, T. Li, arXiv:1709.00692 [hep-ph].
- [34] M. Bordone, C. Cornella, J. Fuentes-Martín, G. Isidori, *Phys. Lett. B* **779**, 317 (2018) [arXiv:1712.01368 [hep-ph]].
- [35] A. Greljo, B.A. Stefanek, *Phys. Lett. B* **782**, 131 (2018) [arXiv:1802.04274 [hep-ph]].
- [36] S.L. Glashow, D. Guadagnoli, K. Lane, *Phys. Rev. Lett.* **114**, 091801 (2015).
- [37] R. Barbieri *et al.*, *Eur. Phys. J. C* **71**, 1725 (2011).
- [38] R. Barbieri, D. Buttazzo, F. Sala, D.M. Straub, *J. High Energy Phys.* **1207**, 181 (2012).
- [39] D.A. Faroughy, A. Greljo, J.F. Kamenik, *Phys. Lett. B* **764**, 126 (2017).
- [40] F. Feruglio, P. Paradisi, A. Pattori, *Phys. Rev. Lett.* **118**, 011801 (2017).
- [41] F. Feruglio, P. Paradisi, A. Pattori, *J. High Energy Phys.* **1709**, 061 (2017) [arXiv:1705.00929 [hep-ph]].
- [42] B. Capdevila *et al.*, *J. High Energy Phys.* **1801**, 093 (2018) [arXiv:1704.05340 [hep-ph]].
- [43] I. Doršner *et al.*, *Phys. Rep.* **641**, 1 (2016).
- [44] A.M. Sirunyan *et al.* [CMS Collaboration], *J. High Energy Phys.* **1707**, 121 (2017) [arXiv:1703.03995 [hep-ex]].
- [45] CMS Collaboration, No. CMS-PAS-SUS-18-001, 2018.
- [46] I. Doršner, A. Greljo, *J. High Energy Phys.* **1805**, 126 (2018) [arXiv:1801.07641 [hep-ph]].
- [47] A. Greljo, D. Marzocca, *Eur. Phys. J. C* **77**, 548 (2017) [arXiv:1704.09015 [hep-ph]].